Mon. Not. R. Astron. Soc. **000**, 1–6 (2015) Printed 23 June 2015 (MN LATEX style file v2.2)

Eötvös Experiments with Supermassive Black Holes

Asha Asvathaman[1], Jeremy S. Heyl[1⋆], Lam Hui[2]
[1] *Department of Physics and Astronomy, University of British Columbia, 6224 Agricultural Road, Vancouver, BC V6T 1Z1, Canada*
[2] *Physics Department, Institute for Strings, Cosmology, and Astroparticle Physics, Columbia University, New York, NY 10027, USA*

Accepted —. Received —; in original form —

ABSTRACT
By examining the locations of central black holes in two elliptical galaxies, M 32 and M 87, we derive constraints on the violation of the strong equivalence principle for purely gravitational objects, *i.e. black holes*, of less than eight percent, $|\eta_N| < 0.08$ from M 32. The constraints from M 87 are substantially weaker but could improve dramatically with better astrometry.

1 INTRODUCTION

The strong equivalence principle (SEP) states that any object regardless of its composition will travel through a gravitational field in the same way. This includes objects with varying contributions of gravitational energy. In particular a black hole whose mass is entirely gravitational should travel in the same manner through the gravitational field as a star. Nordtvedt (1968a,b) argued that metric theories of gravity other than general relativity may exhibit violations of the SEP — in particular, objects which have a large contribution of gravitational energy to their makeup may travel differently through a gravitational field than other objects.

Typically the strong equivalence principle is probed by looking for the Nordvedt effect in the Earth-Moon system or binary stars consisting of a neutron star and a white dwarf (Stairs et al. 2005). The Nordtvedt (1968c) effect results in the polarization of an orbit in the direction of the gravitational acceleration of a large body: the Sun in the case of the Earth-Moon system (Williams et al. 1976; Shapiro et al. 1976), and the Galaxy in the case binary pulsars. The recently discovered millisecond pulsar in a triple system, PSR J0337+1715, will provide further interesting constraints (Ransom et al. 2014).

Here we perform the test proposed by Hui & Nicolis (2012). In particular we will examine the polarization of the orbits of supermassive black holes through the central regions of elliptical galaxies. We will focus on elliptical galaxies because the presence of central black holes is common in sufficiently large elliptical galaxies and the location of the bottom of the graviational potential is straightforward to constrain by determining the centroid of the distribution of stellar light. Interactions between galaxies are ubiquitous, so example systems are straightforward to find. In particular we will examine the small elliptical galaxies that orbit the largest neighbour of the Milky Way galaxy, the Andromeda galaxy or M 31, and the massive elliptical galaxy, M 87, in the Virgo cluster. We will derive an upper limit on SEP violation – how this limit should be interpreted in the context of general gravitational theories will be discussed in §5.

2 CALIBRATION

Let us suppose that we are studying a small stellar system in the gravitational field of a large one. The stars in the small system experience an acceleration toward the centre of the larger one

$$a_\star = \frac{GM}{d^2} \tag{1}$$

where d is the distance between the small system and the larger one and M is the mass of the larger system. These accelerations are typically ten to one hundred times larger than those exerted by large-scale structure $a \sim 600$ km s$^{-1} H_0 \sim 10^{-10}$cm s^{-2}.

Furthermore, let us assume that a massive black hole within the smaller system experiences a different acceleration

$$a_\bullet = (1 - \Delta)\, a_\star \tag{2}$$

where Δ quantifies the extent of violation of the SEP. Nordtvedt (1982) presents an equivalent definition where the ratio of the inertia masses and passive gravitational mass of an object could depend on its constitution and in particular the contribution of gravitational energy,

$$\frac{m_{\rm Gp}}{m_{\rm I}} = 1 - \eta_N \frac{U_{\rm G}}{mc^2}. \tag{3}$$

In the context of the parameterized post-Newtonian treatment of deviations from general relativity (Will 2014),

$$\eta_N = 4\beta\gamma 3\frac{10}{3}\xi - \alpha_1 + \frac{2}{3}\alpha_2 - \frac{2}{3}\zeta_1 - \frac{1}{3}\zeta_2. \tag{4}$$

For the case of a black hole, $U_{\rm G} = mc^2$ so $\Delta = \eta_N$.

The massive black hole also experiences an acceleration due to the stellar system in which it resides. Furthermore, dynamical friction with the less massive stars nearby damps any motion of the black hole relative to its equilibrium position on a short time scale, so absent SEP violation or rare astrophysical effects such as a recent merger or asymetric jets the black hole should lie at the bottom of the gravitational potential well. The effects of individual stellar encounters, Brownian motion, are much smaller than what we discuss here (Broderick et al. 2011).

Near the minimum of the stellar potential we can approximate it as a harmonic oscillator so

$$(1-\Delta)\,\omega^2 x = a_\bullet - a_\star = -\Delta\frac{GM}{d^2} \tag{5}$$

and x is the displacement of the black hole from the centre of the small stellar system in the direction of the larger system. The value of ω depends on the structure of the small stellar system and depends on the mean density within the region surrounding the black hole. For a Hernquist (1990) model for the density distribution that well describes the stellar distribution of elliptical galaxies

$$\rho = \frac{m}{2\pi}\frac{a}{r}\frac{1}{(r+a)^3} \tag{6}$$

where $R_{\rm eff}$, the half-light radius in projection is approximately $1.8153a$. We take the black hole mass to be $m_\bullet = 0.005m$ where m is the mass of the small system, we find that

$$\omega^2 \approx \frac{Gm}{a^3} \tag{7}$$

from n-body simulations that treat perturbation of the stellar system by the black hole in a self-consistent manner. In these simulations we find that small perturbations of the black hole from the centre result in sinusoidal oscillations with this typical frequency, regardless of the number of particles and the softening length adopted, and the amplitude of the perturbation as long as it is smaller than the black hole's sphere of influence. For such small perturbations the black hole pulls the neighbouring stars along with it. The half-mass radius of the Hernquist model is $a/(\sqrt{2}-1)$ so the typical frequency within the half-mass radius is

$$\omega^2 = \frac{4\pi}{8}(\sqrt{2}-1)^3\frac{Gm}{a^3} \approx 0.11\frac{Gm}{a^3}. \tag{8}$$

The oscillation frequency of the black hole is significantly larger than the typical frequency of the system because the black hole lies near the centre of the galaxy where typical density is larger. We will compare this estimate with the detailed measurements of the potential near the core of the elliptical galaxy, M 87, and find good agreement.

If we assume that the black hole lies within a bulge and halo approximately modelled by a Hernquist model (as in van der Marel et al. 1997b), we find that

$$\frac{x}{d} = \frac{\Delta}{1-\Delta}\frac{M}{d^3}\frac{a^3}{m}, \tag{9}$$

so the relative displacement only depends on the relative masses and sizes of the various bodies and the angular displacement does not depend on the distance to the systems from Earth. We can make this explicit by calculating the apparent displacement across the sky as

$$\Delta\theta = \frac{\Delta}{1-\Delta}\frac{M}{\delta^2}\frac{\alpha^3}{m}\cos^3 i \tag{10}$$

where i is the inclination of the line connecting the two bodies with respect to the plane of the sky, δ is the angular distance between the bodies and α is the angular size of the Hernquist radius a of the host galaxy. If smaller galaxies follow an isothermal distribution about the perturbing galaxy as Koch & Grebel (2006) found for the satellites of M 31, the mean value of the geometric term $|\cos^3 i|$ is $4/(3\pi) \approx 0.42$ and the median value is $\sqrt{2}/4 \approx 0.35$. Ninety percent of the time the term lies between 5×10^{-4} and 0.99, so geometric information is especially useful to give firm constraints. Of course the halo of the galaxy group must end somewhere so the lower limit on $\cos^3 i$ found here is somewhat unrealistic. On the other hand if the density of satellites is proportional to r^{-3} like the outer regions of the Navarro-Frenk-White profile (1996), the mean value of the geometric term is $3\pi/16 \approx 0.59$ and the median value is $3\sqrt{3}/8 \approx 0.65$. Ninety percent of the time the term lies between 0.03 and 0.996.

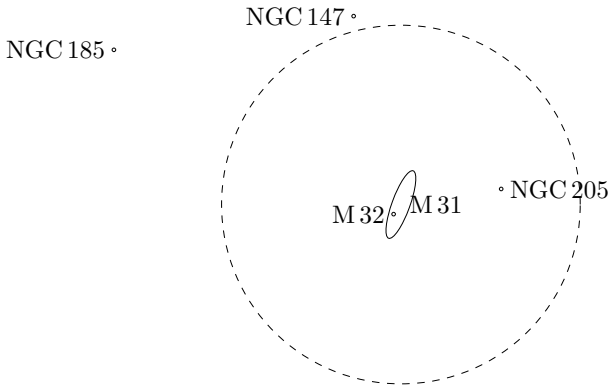

Figure 1. The geometry of the largest elliptical satellite galaxies of the Andromeda Galaxy. The Sun is to 773 kpc to the left of M 32, and the radius of the dashed circle is 100 kpc.

3 THE ANDROMEDA GALAXY SYSTEM

The nearest neighbour of the Milky Way has four small elliptical galaxies orbiting it: M 32, NGC 205, NGC 147 and NGC 185. Fig. 1 depicts the location of the various galaxies relative to each other from the distances compiled by Koch & Grebel (2006). Of course, the distances to the various galaxies are more uncertain than their positions on the sky.

A supermassive black hole (SMBH) has already been discovered in the core of the compact elliptical galaxy M 32 (van der Marel et al. 1997a) and found to be within 0.5 arcseconds of the nucleus of the galaxy (Yang et al. 2015). M 32 is located about 0.4° from the centre of M 31 in the plane of the sky. We can estimate the displacement of the black hole from the centre of M 32 as a function of Δ in the best-case scenario of the minimal separation of M 32 from M 31 of about 5 kpc. In this case M 32 would be well within the halo of M 31, and we could use the circular velocity of M31 of 200 km/s at this distance to estimate the acceleration of M 32 toward the centre of M31, $a_\star$ in Eq. (1),

$$a_\star = \frac{v^2}{d} = 3.6\times10^{-8}\text{cm s}^{-2}. \tag{11}$$

For the galaxy M 32 we take $m = 8\times10^8\text{M}_\odot$ and $R_{\rm eff} = 100$ pc so $a = 55$ pc and

$$x = 0.38\frac{\Delta}{1-\Delta}\text{pc} \tag{12}$$

or

$$\Delta\theta = \frac{x}{d_{\text{M32}-\text{Sun}}} = 0.12\frac{\Delta}{1-\Delta}\text{arcseconds}, \tag{13}$$

so if M 32 lies indeed at the close to minimum distance to M 31, the existing measurement of the position of the black hole yields a constraint; either $\Delta < 0.81$ or $\Delta > 1.3$.

We can improve upon the astrometric constraint of Yang et al. (2015) if we assume that the position of the black hole is coincident with the cusp in the surface brightness of the galaxy. This is a reasonable assumption because the black hole would entrain the neighboring stars, so the stellar nucleus should be centered on the black hole. To measure the possible deviation of the position of the black hole on the sky and the centre of the potential well of the galaxy we use images from the Wide-Field Camera 3 (WFC3) on the Hubble Space Telscope (HST) in the filter, F555W. This instrument features 0.04 arcsecond pixels and a 162×162-arcsecond field of view. Both the Space Telescope Imaging Spectrograph (STIS) and the planetary camera on Wide-Field Planetary Camera 2 (WF/PC2) feature a finer pixel scale but at the expense of field of view. We used images from GO-11714 (PI: Bond) with total exposure time of 120 seconds. To localise the stellar core which lies within the black hole sphere of influence of about 0.3 arcseconds (Joseph et al. 2001), we used circular and elliptical apertures of 0.16 arcseconds and 0.2 arcseconds. To localise the centroid of the outer regions we used two elliptical annuli: one of inner axes 2.8 and 4.3 arcseconds and outer axes of 5.7 and 8.5 arcseconds and one half that size, well outside the black hole's sphere of influence. The centres of the annuli are initially roughly placed within about an arcsecond of the core and updated to lie on the calculated centroid. This is iterated thirty times. The centroids of the various annuli to probe the galactic potential coincide to within 0.01 arcseconds as do the ellipses and circles centered on the stellar cusp, yielding an estimate of the precision of 0.01 arcseconds. Furthermore, the centroid of the cusp and the outer regions also agree to within 0.01 arcseconds. If we combine this constraint with the distance estimate of Koch & Grebel (2006), this yields a constraint $|\Delta| < 0.08$. In fact the maximal distance between M 31 and M 32 consistent with the uncertainties given by Koch & Grebel (2006) is 45 kpc (see also Dierickx et al. 2014, for an alternative interpretation). In the case the constraints on Δ would be much weaker with $\Delta < 0.75$ or $\Delta > 1.5$.

The three smaller elliptical galaxies, NGC 205, NGC 147 and NGC 185, have smaller mass densities and may have more favourable geometry. However, SMBHs have not yet been identified in these galaxies. Each of these galaxies has a mass of about $2 \times 10^8 M_\odot$ and a $R_{\rm eff} \approx 300$ pc, so $a \approx 165$ pc. The two galaxies, NGC 147 and NGC 185 are each about 100 kpc from M31, so the enclosed halo mass is about $10^{12} M_\odot$. This yields a typical value of the displacement of

$$x = 2.3 \frac{\Delta}{1-\Delta} \text{pc and } \Delta\theta = 0.75 \frac{\Delta}{1-\Delta} \text{arcseconds..} \qquad (14)$$

Although NGC 205 may be somewhat closer to M 31 at 50 kpc than the other galaxies, the geometry is somewhat poorer according to the distance given by Koch & Grebel (2006) perhaps reducing the angular displacement by a factor of two counteracting the increased acceleration. This yields a similar observed displacement. If a SMBH is discovered near the centre of these galaxies and can be localised within 0.5 arcseconds, this would yield a constraint of $-2.0 < \Delta < 0.4$.

On the other hand, NGC 205 may lie at the same distance from us as M 31. This is consistent with the errorbars given by Koch & Grebel (2006). Furthermore, Geha et al. (2006) argue that NGC 205 is interacting tidally with M 31, favouring this interpretation. At this minimum possible distance to M 31 of about 7 kpc, and we obtain a much larger linear and angular displacement

$$x = 43. \frac{\Delta}{1-\Delta} \text{pc and } \Delta\theta = 13. \frac{\Delta}{1-\Delta} \text{arcseconds.} \qquad (15)$$

In this most favourable case the constraint would be $|\Delta| < 0.04$ with 0.5-arcsecond astrometry and $|\Delta| < 8 \times 10^{-3}$ with 0.01-arcsecond astrometry.

4 VIRGO ELLIPTICAL GALAXIES

One of the largest elliptical galaxies in the Virgo Cluster, M 87, also contains a supermassive black hole and lies at the centre of the Virgo A subcluster which contains the bulk of the mass of the Virgo Cluster, about $10^{14} M_\odot$. The Virgo Cluster is still in the process of forming and contains at least two additional subclumps of masses of about $10^{13} M_\odot$. The subclump closest to M 87 is centered on M 84 and M 86 about 1.3° away. M 89 is also a similar angular distance away, so this analysis applies to it as well, but it is likely to be less massive.

For the galaxy M 87 we take $R_{\rm eff} = 164''$ (Ferrarese et al. 2006) so $a = 90''$. We will take the mass of M 87 to be about $4 \times 10^{12} M_\odot$ (Wu & Tremaine 2006) and take the mass of the subclump containing M 84 and M 86 to be $10^{13} M_\odot$ at a distance of 1.3°. This yields a displacement of

$$\Delta\theta = 0.08 \cos^3 i \frac{\Delta}{1-\Delta} \text{arcseconds.} \qquad (16)$$

We can examine the stellar distribution of M 87 in further detail. Ferrarese et al. (2006) find that the central region of M 87 is better fit by a "core-Sérsic" model (Sérsic 1968; Trujillo et al. 2004) that has a much less cuspy central surface brightness distribution than a Hernquist model. The break radius between the core and the outer Sérsic model is about 7 arcseconds.

Walsh et al. (2013) determine the mass of the central black hole of M 87 to be about $3.5 \times 10^9 M_\odot$ (approximately 10^{-3} of the mass of the galaxy) and to dominate the mass within about 5.61 arcseconds of the centre. They also model the contribution of the stellar mass to the circular velocity in this inner region, yielding a value of about 160 km/s at $4''$ from the black hole consistent with the photometry of Ferrarese et al. (2006) and a mass-to-light ratio of 4. Assuming a smaller mass-to-light ratio would yield smaller constraints on Δ, roughly the expected displacement for a given value of Δ is inversely proportional to the square of the mass-to-light ratio. As the stellar mass-to-light ratio decreases, the effect of the stellar potential diminishes, increasing the displacement, and the sphere of influence of the black hole increases, so we can probe the effect at larger radii from the black hole, further increasing the expected displacement.

Within 10 arcseconds the black hole contributes about thirty percent of the mass, so we will use the circular velocity due to the stellar contribution at this radius of about 210 km/s to estimate the displacement of the black hole due to SEP violation. Using a distance to M 87 of 16.4 Mpc (Bird

et al. 2010) and the same mass and angular distance to the subclump centred on M 84 as earlier yields

$$x = 4.6\frac{\Delta}{1-\Delta}\cos^2 i \text{ pc} \quad (17)$$

and

$$\Delta\theta = 0.06\frac{\Delta}{1-\Delta}\cos^3 i \text{ arcseconds} \quad (18)$$

where we have extrapolated the theoretical stellar mass profile of Walsh et al. (2013) out to 10 arcseconds, slightly beyond the break radius of 7.15 arcseconds determined by Ferrarese et al. (2006) where the surface brightness profile steepens.

The position of the black hole can in principle be determined to microarcsecond precision with microwave interferometry (Broderick et al. 2011). On the other hand, the centre of the potential well is best defined in the optical using the isophotes of the galaxy. Fortunately, the supermassive black hole is also apparent in the optical. The innermost isophotes will be centered on the black hole because it will dominate the potential well, so the centres of more distant isophotes provide an estimate of the potential well that constrains the black hole.

Batcheldor et al. (2010) argued from isophotal analysis of observations with the Advanced Camera for Survey on HST that the AGN may be displaced from the centre of the galaxy by about 7 pc in a direction opposite to the observed jet (about 0.1 arcseconds). However, subsequently neither Gebhardt et al. (2011) nor Walsh et al. (2013) found evidence for displacement greater than about one parsec; the position determined by Gebhardt et al. (2011) was consistent with that of Batcheldor et al. (2010) within the larger errorbars of Gebhardt et al. (2011). Batcheldor et al. (2010) outlined several astrophysical explanations for a potential displacement such as a SMBH binary, a recent merging of black holes or a one-sided jet. The interaction with the neighbouring stars or even clusters of stars is too weak to explain such a displacement.

To measure the possible deviation of the position of the black hole on the sky and the centre of the potential well of the galaxy we use images from the Wide-Field Camera 3 (WFC3) on the Hubble Space Telscope (HST) in the ultraviolet filter, F225W. We used images from GO-12989 (PI: Renzini) with total exposure time of 5599 seconds as depicted in Fig. 2. To find the centre of the potential we calculated the light centroid within three circular annuli of inner and outer radii 24 and 36 arcseconds, 12 and 24 arcseconds, and 9 and 15 arcseconds. M 87 is an E0 galaxy so its isophotes are nearly circular (Ferrarese et al. 2006). If we take the mass of the black hole to be about $4 \times 10^9 M_\odot$, it will dominate the mass within about 6.6 arcseconds from the centre. Within 12 arcseconds it contributes less than 25% of the mass, and within 24 arcseconds it contributes about 8% of the mass; therefore, these annuli lie outside the black hole's sphere of gravitational influence. The slices of the annulus along the direction of the observed jet and potential counterjet are omitted from the calculation and so exclude light from the AGN itself. This technique contrasts with that of Batcheldor et al. (2010). They explicitly masked the noticable jet emission as well as globular clusters. Here we remove a much larger region from the analysis both in the direction of the jet and the opposite direction. This excludes both the observed jet and a wide regions around the jets. The excluded region is symmetric, so we minimize any potential bias along the jet axis. Furthermore, the measurements that we use are in F225W with a higher angular resolution camera (WFC3 vs. ACS). In this ultraviolet filter, the emission from globular clusters is negligible. The centre of the annuli are initially roughly placed within about an arcsecond of the AGN and updated to lie on the calculated centroid. This is iterated thirty times.

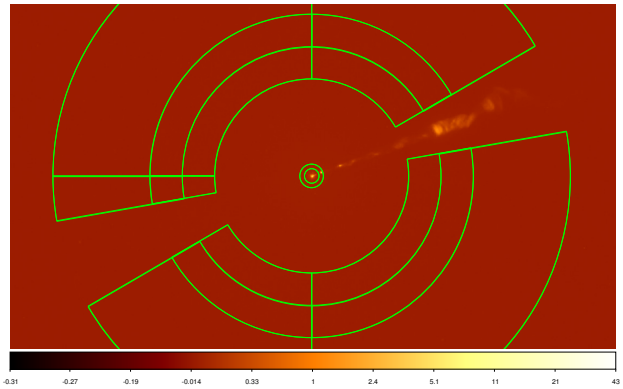

Figure 2. Central region of M 87 focussing on the AGN. Several apertures to determine the centroid of the light are depicted. The two middle annuli lie from 9 to 15 arcseconds and 12 to 24 arcseconds from the centre. The inner apertures are circular and 0.15 and 0.2 arcseconds in radius. The outermost aperture between 24 and 36 arcseconds is not depicted.

To determine the location of the black hole we performed a similar centroiding on circular apertures of 0.15 and 0.2 arcseconds, also initially centred on the AGN within 0.2 arcseconds. We have repeated this process several times using different starting positions, resulting in slightly different centroids all consistent within their mutual standard deviation of 0.03 arcseconds, slightly less than a pixel. This is consistent with the precision found by Walsh et al. (2013) and poorer than we found with M 32 because the surface brightness profile of M 87 is much shallower. The isophotes constrain the deviation of the black hole from the centre of the potential within 0.03 arcseconds, yielding a constraint on the violation of the SEP for black holes of $-1 < \Delta < 0.3$, assuming the more conservative displacement estimate Eq. (18) and a favourable geometry of $i \approx 0°$. Using additional images, more sophisticated isophote fitting procedure and more detailed modelling of the mass distribution of the Virgo cluster could possibly yield smaller constraints.

5 CONCLUSIONS

How does our limit on Δ fit within the context of existing scalar-tensor theories? SEP violation occurs in these theories because compact objects have a suppressed scalar charge, leading to a weaker scalar coupling to the environment. For the classic Brans-Dicke theory, solar system tests constrain the scalar-matter coupling to be fairly weak to begin with (much weaker than tensor-matter), thus predicting SEP violation that is much below our limit. More recent scalar-tensor theories open up the interesting possibility of predict-

ing observable SEP violation on large scales while respecting the solar system constraints – the latter is achieved by what is known as screening mechanism. Screening introduces a subtlety in the interpretation of Δ, however – it becomes scale/environment dependent. In the case of the M32-M31 system, we estimate $\Delta \sim 10^{-3}$ in galileon theories (Nicolis et al. 2009). For such theories, $\Delta \sim 1$ can be found in situations where the acceleration is due to large scale structure, quite a bit smaller than the acceleration of our setup (Hui & Nicolis 2012). Despite this, deriving a phenomenological limit on Δ is useful, for several reasons.[1] First, new theories – massive gravity being an example – are still being developed. Second, equivalence principle violation remains to be worked out even for some existing theories (Hui et al. 2009). Third, this type of galaxy-satellite system constraint on Δ can be improved.

Both the calibration and observational analysis presented here can be improved upon in several directions. From the calibration standpoint, we have considered just the force on the black hole and not the cotery of stars in its immediate gravitational influence. Moving the black hole from the centre of the stellar system will also move these stars, somewhat diluting the Nordvedlt effect. Of course in the simulations that we did perform as the black hole oscillates about the centre of mass of the stellar system, it carries the neighbouring stars with it, but additional study is warranted where one would start the black hole in the centre of the galaxy increase the differential acceleration, say due to the effect of the small galaxy approaching the larger one, and determine where the black hole ends up.

As we have mentioned earlier, there are more sophisticated ways to determine the centre of the galaxy with isophotal fitting and by considering measurements from several observations at several wavelengths. In principle one could find tighter constraints on the deviation of the black hole from the centre of the potential. In the case of M 32 the existing constraints are just 0.5 arcseconds because one has to link the radio coordinate system to the visual one. These could possibly be improved dramatically with further observations. The visual core of M 32 lies within 0.01 arcseconds of the centroid of the outer isophotes of the galaxy, indicating that if the black hole is coincident with the core, $|\eta_N| < 0.08$, competitive with the results from pulsar timing (Stairs et al. 2005).

Furthermore, the discovery of a supermassive black hole in one of the other elliptical satellites of M 31 could provide stronger constraints from the M 31 system. However, the main uncertainty in the constraints comes from the unknown geometry of the system as we saw for M 32 in particular so further information on the relative distances of the various galaxies would yield better constraints on the results. Perhaps other interacting and nearly interacting galaxies in the local Universe could also provide more information and would statistically limit the violation of SEP in the motion of black holes.

The constraint on SEP from the motion of black holes probes the SEP in an essentially different limit from that of lunar ranging; however, the technique outlined here could become competitive with the lunar ranging results which now constrain $|\eta_N| < 1.3 \times 10^{-3}$ (Baeßler et al. 1999; Adelberger 2001). Improved astrometric measurements of the centre of the potential of M 87 and the location of the black hole could be achieved with existing visual and UV data and the position of the black hole could be constrained further with radio interferometry provided the optical and radio astrometry could be tied together with sufficient precision. Relative astrometry with a precision $\sim 10^{-4}$ arcseconds can be achieved with Hubble photometry (e.g. Heyl et al. 2012), a factor of one hundred better than presented here, so constraints on $|\eta_N|$ of 10^{-3} could be possible with supermassive black holes. If microarcsecond astrometry can be brought to bear (e.g. Broderick et al. 2011) on M 87, then constraints on η_N on the order of 10^{-4} might be possible.

This research is based on NASA/ESA Hubble Space Telescope observations obtained at the Space Telescope Science Institute, which is operated by the Association of Universities for Research in Astronomy Inc. under NASA contract NAS5-26555 and accessed through the Hubble Legacy Archive. These observations are associated with proposal GO-11714 (PI: Bond) and GO-12989 (PI: Renzini). This work was supported by the Natural Sciences and Engineering Research Council of Canada, the Canadian Foundation for Innovation, the British Columbia Knowledge Development Fund, the Department of Energy and NASA. LH thanks Henry Tye and the HKUST Institute for Advanced Study for hospitality.

[1] Note also the environmental dependence of Δ is often such that Δ on the left hand side of Eq. (5) is much smaller than Δ on the right; the statements above refer to the latter.

REFERENCES

Adelberger, E. G. 2001, Classical and Quantum Gravity, 18, 2397

Baeßler, S., Heckel, B. R., Adelberger, E. G., , Gundlach, J. H., Schmidt, U., & Swanson, H. E. 1999, Phys. Rev. Lett., 83, 3585

Batcheldor, D., Robinson, A., Axon, D. J., Perlman, E. S., & Merritt, D. 2010, Astrophys. J. Lett., 717, L6

Bird, S., Harris, W. E., Blakeslee, J. P., & Flynn, C. 2010, Astron. Astrophys., 524, A71

Broderick, A. E., Loeb, A., & Reid, M. J. 2011, Astrophys. J., 735, 57

Dierickx, M., Blecha, L., & Loeb, A. 2014, Astrophys. J. Lett., 788, L38

Ferrarese, L., Côté, P., Jordán, A., Peng, E. W., Blakeslee, J. P., Piatek, S., Mei, S., Merritt, D., Milosavljević, M., Tonry, J. L., & West, M. J. 2006, Astrophys. J. Suppl., 164, 334

Gebhardt, K., Adams, J., Richstone, D., Lauer, T. R., Faber, S. M., Gültekin, K., Murphy, J., & Tremaine, S. 2011, Astrophys. J., 729, 119

Geha, M., Guhathakurta, P., Rich, R. M., & Cooper, M. C. 2006, Astron. J., 131, 332

Hernquist, L. 1990, Astrophys. J., 356, 359

Heyl, J. S., Richer, H., Anderson, J., Fahlman, G., Dotter, A., Hurley, J., Kalirai, J., Rich, R. M., Shara, M., Stetson, P., Woodley, K. H., & Zurek, D. 2012, Astrophys. J., 761, 51 (25 pages)

Hui, L. & Nicolis, A. 2012, Physical Review Letters, 109, 051304

Hui, L., Nicolis, A., & Stubbs, C. W. 2009, Physical Review D, 80, 104002
Joseph, C. L., Merritt, D., Olling, R., Valluri, M., Bender, R., Bower, G., Danks, A., Gull, T., Hutchings, J., Kaiser, M. E., Maran, S., Weistrop, D., Woodgate, B., Malumuth, E., Nelson, C., Plait, P., & Lindler, D. 2001, Astrophys. J., 550, 668
Koch, A. & Grebel, E. K. 2006, Astron. J., 131, 1405
Navarro, J. F., Frenk, C. S., & White, S. D. M. 1996, Astrophys. J., 462, 563
Nicolis, A., Rattazzi, R., & Trincherini, E. 2009, Physical Review D, 79, 064036
Nordtvedt, K. 1968a, Physical Review, 169, 1014
—. 1968b, Physical Review, 169, 1017
—. 1968c, Physical Review, 170, 1186
Nordtvedt, Jr., K. 1982, Reports on Progress in Physics, 45, 631
Ransom, S. M., Stairs, I. H., Archibald, A. M., Hessels, J. W. T., Kaplan, D. L., van Kerkwijk, M. H., Boyles, J., Deller, A. T., Chatterjee, S., Schechtman-Rook, A., Berndsen, A., Lynch, R. S., Lorimer, D. R., Karako-Argaman, C., Kaspi, V. M., Kondratiev, V. I., McLaughlin, M. A., van Leeuwen, J., Rosen, R., Roberts, M. S. E., & Stovall, K. 2014, Nature, 505, 520
Sérsic, J. L. 1968, Atlas de galaxias australes (Cordoba, Argentina: Observatorio Astronomico)
Shapiro, I. I., Counselman, III, C. C., & King, R. W. 1976, Physical Review Letters, 36, 555
Stairs, I. H., Faulkner, A. J., Lyne, A. G., Kramer, M., Lorimer, D. R., McLaughlin, M. A., Manchester, R. N., Hobbs, G. B., Camilo, F., Possenti, A., Burgay, M., D'Amico, N., Freire, P. C., & Gregory, P. C. 2005, Astrophys. J., 632, 1060
Trujillo, I., Erwin, P., Asensio Ramos, A., & Graham, A. W. 2004, Astron. J., 127, 1917
van der Marel, R. P., de Zeeuw, P. T., Rix, H.-W., & Quinlan, G. D. 1997a, Nature, 385, 610
van der Marel, R. P., Sigurdsson, S., & Hernquist, L. 1997b, Astrophys. J., 487, 153
Walsh, J. L., Barth, A. J., Ho, L. C., & Sarzi, M. 2013, Astrophys. J., 770, 86
Will, C. 2014, Living Rev. Relativity, 17, 4, (accessed 16 May 2015): http://www.livingreviews.org/lrr-2014-4
Williams, J. G., Dicke, R. H., Bender, P. L., Alley, C. O., Currie, D. G., Carter, W. E., Eckhardt, D. H., Faller, J. E., Kaula, W. M., & Mulholland, J. D. 1976, Physical Review Letters, 36, 551
Wu, X. & Tremaine, S. 2006, Astrophys. J., 643, 210
Yang, Y., Li, Z., Sjouwerman, L. O., Wang, Q. D., Gu, Q., Kraft, R. P., & Yuan, F. 2015, ArXiv e-prints